Chapter 6

Carbonation Simulation Model

6.1 Model Considerations

As soon as water is brought into contact with Portland cement, the cement constituent compounds undergo a series of chemical reactions, called hydration reaction. The hydration reaction produces calcium hydroxide as one of the products. Calcium hydroxide beneficially provides alkalinity in concrete pores. When fly ash is used in concrete, the pozzolanic reaction consumes the released calcium hydroxide. However, the pozzolanic reaction affects only some amount of calcium hydroxide. When the atmospheric carbon dioxide diffuses into concrete, it reacts with the dissolved calcium hydroxide and can significantly reduce the alkalinity of the pore solution in the carbonated part of the concrete. The chemical reaction that characterizes the carbonation reaction is generally described as follow.

$$Ca(OH)_2 + CO_2 \rightarrow CaCO_3 + H_2O \qquad (6.1)$$

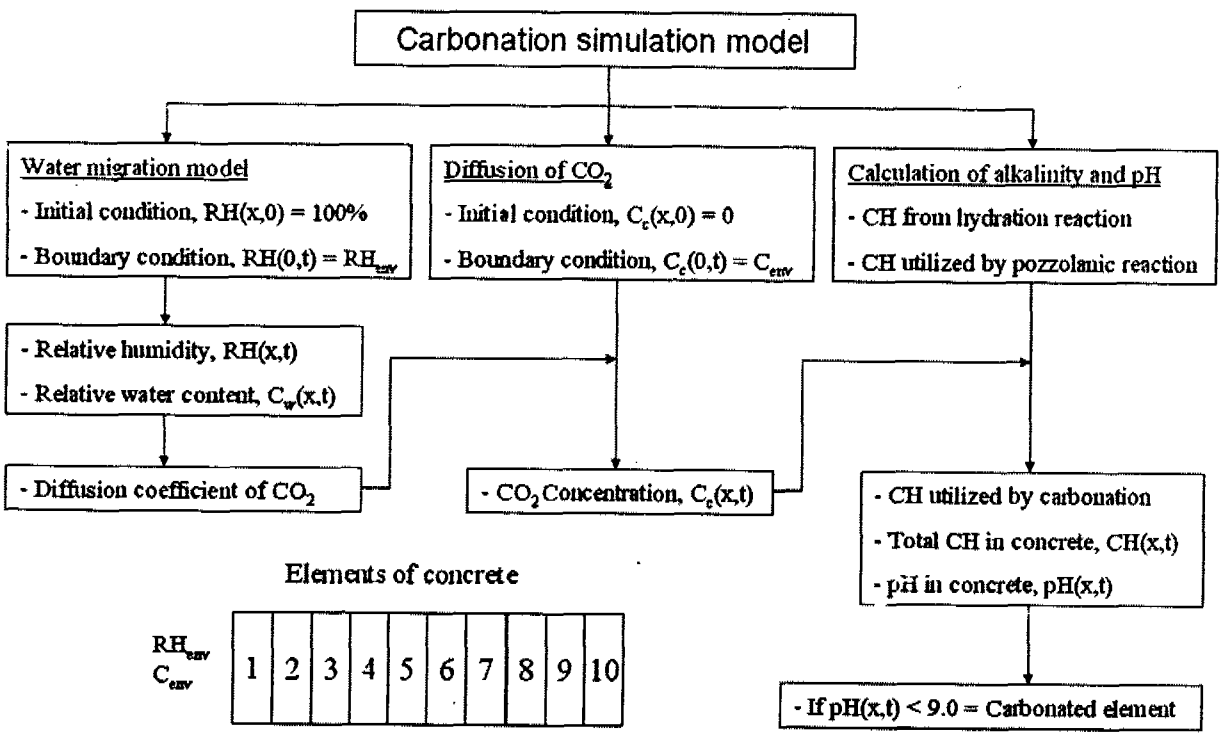

Note: RH_{env} and C_{env} are the relative water content and carbon dioxide concentration in the environment

Fig. 6.1 Flow chart of the model for simulating corrosion of reinforcing steel due to carbonation

The mathematical model proposed in this study was developed for one-dimensional simulation since carbonation is considered as a near surface problem. The rate of gas diffusion is assumed to follow the Fick's law, which is popularly used to describe a motion

by the diffusion of a substance in the concrete in the direction of the concentration gradient. The effects of pore water and relative humidity in the pores on the carbonation phenomenon are also significant. The degree of saturation and humidity in the pores greatly influences the diffusion of carbon dioxide. This is because in saturated concrete, the pores are filled with water and the carbon dioxide diffusion is almost impossible. Carbon dioxide starts diffusing when the water in concrete pore dries out. The water content of the concrete can be estimated by the water migration model developed herein. In this study, the model for simulating carbonation (carbonation simulation model) includes water migration model, carbon dioxide diffusion, and calculation of alkalinity and pH in concrete pore water. Fig. 6.1 illustrates the flow chart showing the processes of the model. The computations were based on several reactions and diffusion processes.

6.2Water Migration Model

6.2.1 Model Formulation

The water movement in concrete is involved in many deterioration processes of concrete, such as drying shrinkage, carbonation, and chloride-induced corrosion. The movement of water in concrete is usually caused by one or a combination of the transportation mechanisms which include water vapor diffusion due to the vapor concentration gradient within concrete, the sorptivity caused by capillary suction, and the permeability due to the hydraulic pressure gradient (Wong et al. 2001, CEB 1989). The permeability is not considered herein because carbonation is generally not serious in situations under hydraulic pressure where concrete is usually saturated with water. The saturated condition is also assumed during raining due to the sorptivity. Thus, the water vapor diffusion behavior is modeled herein. After curing, concrete is generally saturated. When concrete is subjected to drying, water in concrete is considered to migrate through the system of interconnected capillary pores according to the gradient of vapor pressure which is regarded to vary linearly with relative humidity in the pore of concrete. The rate of vapor movement can be derived by adopting the Fick's Law as follow (Rose 1965, Crank 1975, Tangtermsirikul et al 1992).

$$FH(x,t) = -DH(x,t)\frac{\partial RH(x,t)}{\partial x} \tag{6.2}$$

where FH is the flux of vapor transfer across a unit cross-sectional area of concrete ($kg/m^2/day$). DH is the apparent diffusion coefficient of vapor (kg/m/day). RH is the relative humidity in concrete pores (%). x is the distance from the exposed surface (m). However, it is difficult to measure directly the relative humidity in concrete. The relative humidity in concrete was reported to have relationship with relative water content in concrete (CEB 1989, Saeki et al. 1991, Maruya et al. 1992). In this study, the similar relationship was utilized as shown in Fig. 6.2. This relationship is based on the condition that vapor phase is in equilibrium with liquid phase and is adopted herein for the numerical analysis.

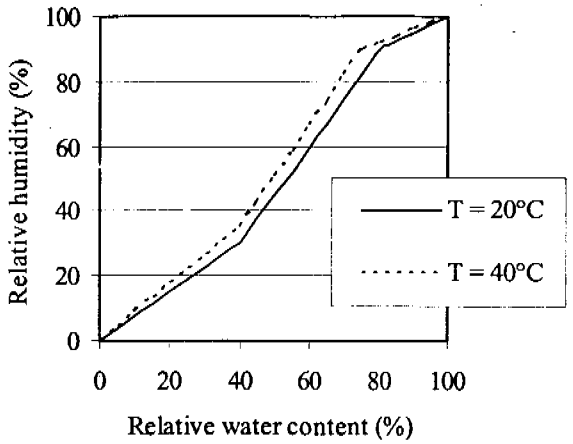

Fig. 6.2 Relationship between relative humidity and relative water content in concrete

6.2.2 Relative water content

The relative water content is defined as the percentage of the amount of evaporable water in concrete at a specified time to the amount of evaporable water in the saturated concrete. Under an assumption that concrete is saturated before drying begins, $W_e(x,0) = W_{sat}(x,0)$, then

$$C_w(x,t) = 100 \times \frac{W_e(x,t)}{W_{sat}(x,t)} \tag{6.3}$$

in which, from the mass balance equation,

$$W_e(x,t) = W_{sat}(x,t) - \int_0^t [FH(x,t) - FH(x+1,t)]Adt \tag{6.4}$$

where C_w is the relative water content (%).W_e is the amount of evaporable water in concrete at a specified time and distance from the exposed surface (kg). W_{sat} is the amount of evaporable water in saturated concrete (kg). A is the considered cross sectional area (m^2). FH(x, t) is the flux of vapor transfer from element x to the next outer element (x-1) and FH(x+1, t) is the flux of vapor transfer from the inner element (x+1) to element x as seen in Fig. 6.3.

The evaporable water means the free water present in the capillary pore and unbound in the cement paste. The physically bound water or gel water is an amount of non-evaporable water that is adsorbed on the surface of the gel solid (Powers 1960, Jensen and Hansen 2001). During the hydration and pozzolanic reactions, the free (evaporable) water decreases with an increase in the degree of reactions because some water is used in the reactions and entrapped in the products of the reactions. W_{sat} is the free water in the saturated concrete and is formulated by Tangtermsirikul and Saengsoy (2002, see Appendix A3) to have relationship with the average degree of reaction (see Figs 6.4 and 6.5 as examples). The average degree of reaction is derived form Eq. 3.11.

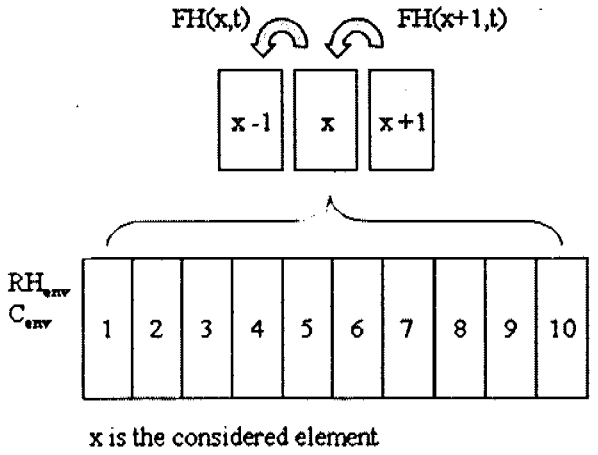

Fig. 6.3 Diagram for showing the flux of water movement in concrete

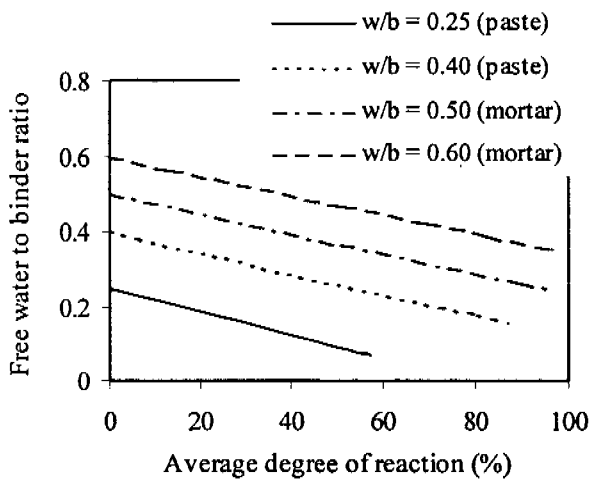

Fig. 6.4 Weight ratio of free water per total binder of cement-only mixtures

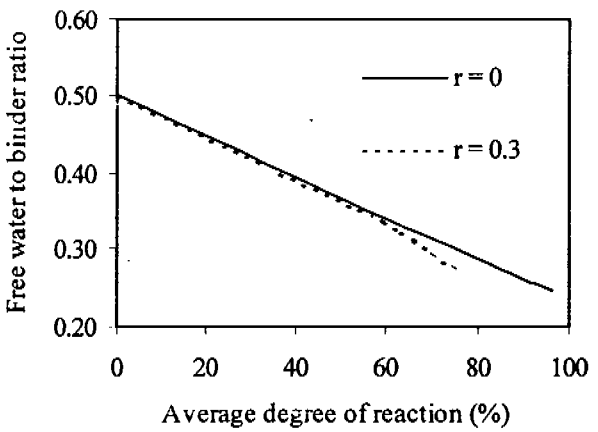

Fig. 6.5 Weight ratio of free water per total binder of cement-fly ash mortar (w/b = 0.5)

6.2.3 Diffusion coefficient of water vapor

The diffusion of water vapor is controlled mainly by the pore characteristics and the relative water content in the pores. The pore characteristics are described herein by total porosity and average pore size. The diffusion rate of gas is higher in a more porous concrete. For the same porosity, the diffusion rate of gas is higher when the concrete has a larger average pore size. The water content in the pores is considered to obstruct the diffusion of gases. In addition, the diffusion is also affected by the boundary effect, i.e. the water vapor movement between the exposed surface element and the environment is easier than the movement within the concrete. The equations for obtaining diffusion coefficient of water vapor through concrete were formulated from the back analysis of the experimental results of relative water content using Eq. (6.2), (6.3), and (6.4) as follows.

$$DH_0(t) = 1.19\times10^{-3}\, d(t)\, n(t)^{(1.6wb-1.6)}\, \frac{\eta}{C_w^{0.11}(x,t)} \tag{6.5a}$$

$$DH_i(t) = 1.16\times10^{-3}\, d(t)\, n(t)^{(1.6wb-1.6)}\, \frac{\eta}{C_w^{0.11}(x,t)} \tag{6.5b}$$

where DH_o is the diffusion coefficient at the exposed surface and DH_i is the diffusion coefficient of the inner concrete (kg/m/day). wb is the water to total binder ratio. C_w is the relative water content in pore of concrete element (%). n and d are the total porosity (%) and the average pore size (nm) of cementitious matrix, respectively. η is the effect of aggregate content. The total porosity (n) and the average pore size (d) of cementitious matrix were formulated to have relationship with the average degree of reaction by Sumranwanich and Tangtermsirikul (2003) as in Figs. 6.6 and 6.7 as examples (see Appendix A4). The difference of diffusion coefficient of the exposed surface from that of inner concrete can be considered to be due to two major facts, i.e. the boundary effect that makes the surface portion richer in paste and less continuity in aggregate location than the inner portion and the open boundary outside the concrete surface makes the substances move more freely and conveniently out of and into the concrete.

The effect of aggregate content was simply formulated under an assumption that diffusion coefficient of the normal aggregate is much smaller than that of the paste as follow.

$$\eta = \frac{V_p}{V_t} \tag{6.6}$$

where V_p and V_t are the volume of paste in the concrete and the total volume of concrete, respectively (m^3/m^3 of concrete). It is realized that scientifically, transition zone has some contribution on the diffusion process to a certain extent. However, at this state, the effect of transition zone was still not taken into account in the model.

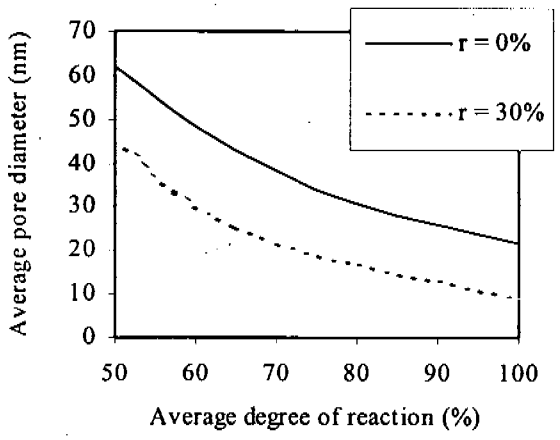

Fig. 6.6 Average pore diameter of paste (w/b = 0.4)

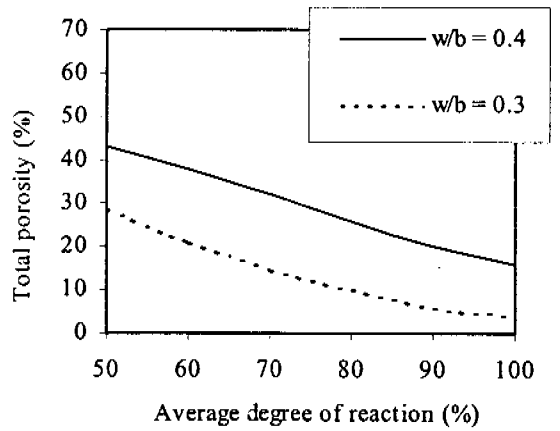

Fig. 6.7 Total porosity of cement-only paste

6.2.4 Verifications

The water migration model is verified by using the test results of relative water content distribution tested in this study. The experimental program and results are given in sections 4.6 and 5.5, respectively. The test results of relative water content (C_w) were compared, in Fig. 6.8 to 6.10, with results calculated from the model. Fig. 6.8 illustrated the comparison of relative water content at different water to binder ratio and fly ash content. It was found that the water migration rate of the specimen was higher for a higher water to binder ratio. The increase of fly ash content tends to increase the water migration rate. Fig. 6.9 shows the comparison of relative water content at different drying condition (40 °C with 55% RH and 30 °C with 65% RH) and fly ash content. It was found that the migration rate of water increases (lower relative water content) when the humidity decreased and the temperature increased. In addition, Fig. 6.10 demonstrated the effect of fly ash content on the distribution of relative water content in no-sand concrete. From Figs 6.8 to 6.10, it can be concluded that the proposed model can be used to estimate the relative water content distribution in mixture with satisfactory accuracies.

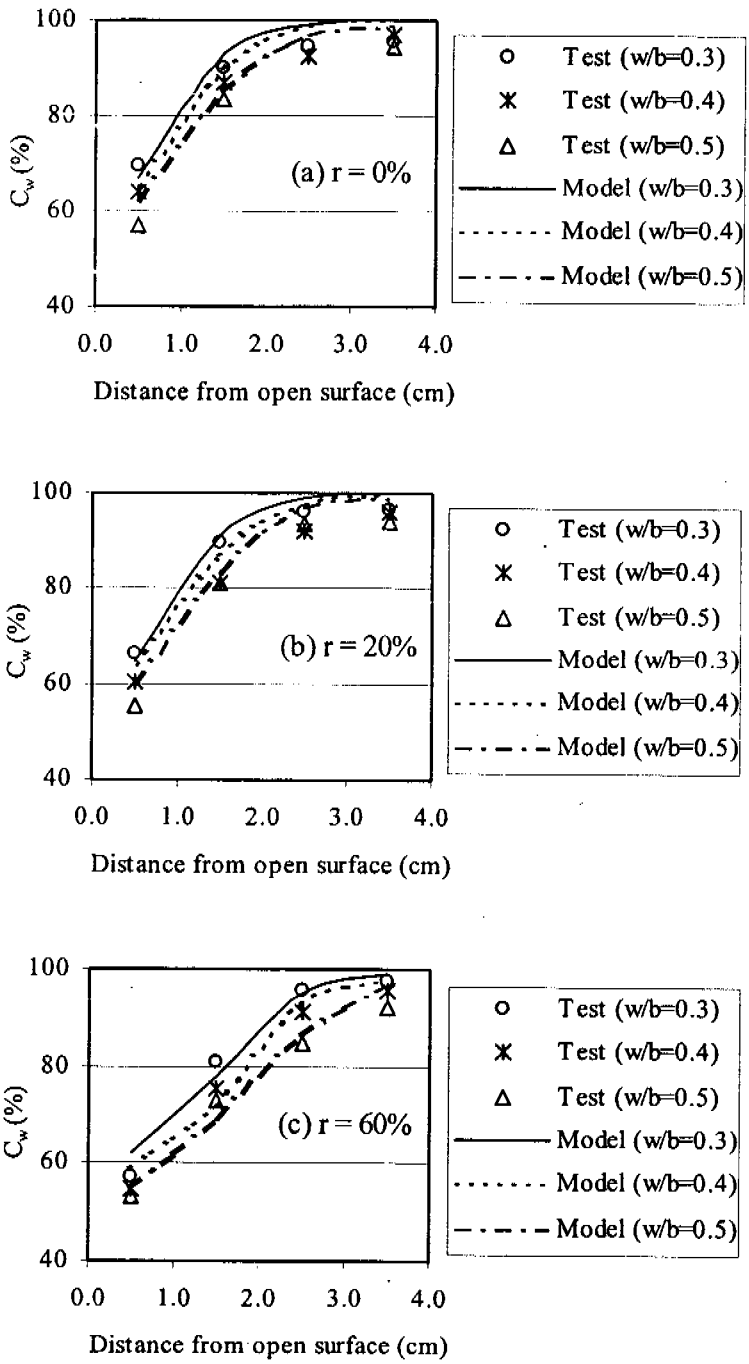

Fig. 6.8 Relative water content in mortar (cured and dried for 28 days)

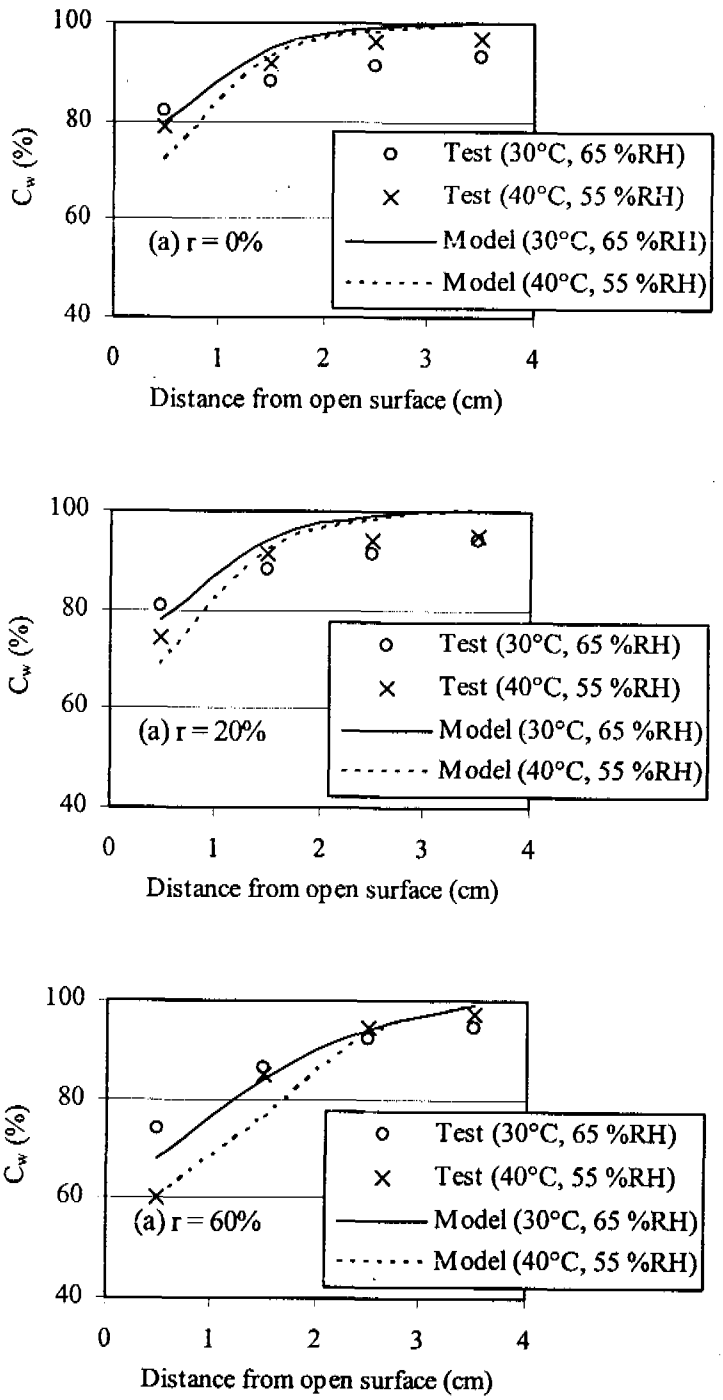

Fig. 6.9 Relative water content in paste (cured and dried for 28 days)

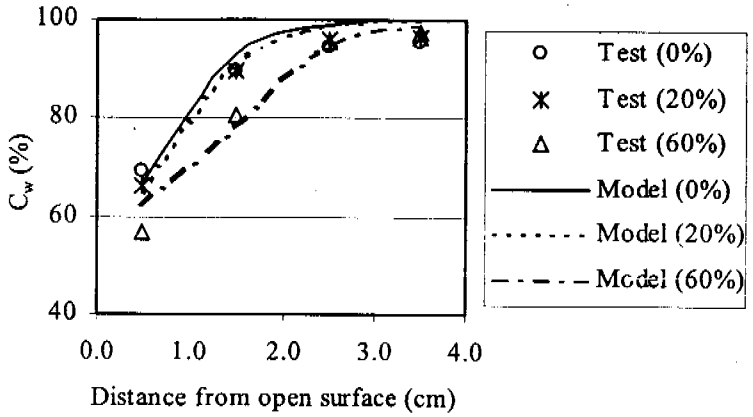

Fig. 6.10 Relative water content in no-sand concrete (w/b = 0.4, cured and drying for 28 days)

6.3 Diffusion of Carbon Dioxide

Carbon dioxide in environment starts diffusing effectively into concrete after the water in concrete dries out. The concentration gradient of carbon dioxide acts as the driving force. The movement of carbon dioxide through the interconnected pores in concrete also follows the Fick's law and can be derived as in Eq. (6.7). It is remarked that the diffusion of the dissolved carbon dioxide is neglected.

$$F_c(x,t) = -D_c(x,t)\frac{\partial C(x,t)}{\partial x} \tag{6.7}$$

where F_c is the flux of carbon dioxide diffusing across a unit cross-sectional area of concrete (mol/m^2/day). D_c is the diffusion coefficient of carbon dioxide (m^2/day). C is the concentration of carbon dioxide in gas phase in the pores in moles of carbon dioxide per unit volume of air space in the pores (mol/m^3 of air space in pores). The volume of air space in pores in each element of concrete is derived from

$$V_a(x,t) = \left[1 - \frac{C_w(x,t)}{100}\right]\frac{n(t)}{100} A\,\Delta x \tag{6.8}$$

where V_a is the volume of air space in the concrete pores (m^3). C_w is the relative water content (%). n is the total porosity (%). A is the cross-sectional area of the element (m^2). Δx is the thickness of the element (m). Similar to the diffusion coefficient of water vapor, the diffusion coefficient of carbon dioxide depends on pore characteristics of concrete, relative water content in concrete, and boundary effect. In addition, relative humidity in pores is also considered affecting the diffusion of carbon dioxide. The higher relative humidity is the lower the carbon dioxide diffusion will be. The diffusion coefficient of carbon dioxide is formulated by back analysis of the test results of carbonation depth as follows

$$D_{co} = \frac{8.3\times10^{-7} d(t) n^2(t) \eta}{RH(x,t)}\left[1 - \frac{C_w(x,t)}{100}\right] \tag{6.9a}$$

$$D_{ci} = \frac{6.4\times10^{-7} d(t) n^2(t) \eta}{RH(x,t)} \left[1 - \frac{C_w(x,t)}{100}\right] \quad (6.9b)$$

where D_{co} and D_{ci} are the diffusion coefficient of carbon dioxide of the exposed surface and the inner concrete element, respectively (m^2/day). n and d are the total porosity (%) and the average pore size (nm), respectively, of the cementitious matrix. RH and C_w are the relative humidity (%) and the relative water content (%), respectively, in concrete pores. η is the effect of aggregate content, which can be obtained form Eq. (6.6).

6.4 Calculation of Alkalinity and pH in Concrete Pore Water

6.4.1 Calcium Hydroxide in Concrete

When hydration of C_3S and C_2S takes place, the reaction produces calcium silicate hydrate (CSH) with the released lime separating out as calcium hydroxide (CH). The released CH becomes available for the process of the pozzolanic reaction and also for the carbonation reaction. The amount of CH in non-carbonated concrete can be computed as follow.

$$CH_t(x,t) = CH_{gh}(x,t) - CH_{cp}(x,t) \quad (6.10)$$

where CH_t, CH_{gh}, and CH_{cp} are the total amount of CH, CH generated by hydration reaction, and CH utilized by pozzolanic reaction, respectively (in term of weight, kg) in the considered element x at the considered time t (day).

(i) Calcium Hydroxide generated by Hydration Reaction

C_3S and C_2S are believed to be the main producer of the CH. The amount of CH is controlled mainly by their hydration rates. By making an approximate assumption that $C_3S_2H_3$ and CH are the products of both C_3S and C_2S. The reactions of hydration of C_3S and C_2S can be written as follows.

$$2C_3S + 6H \rightarrow C_3S_2H_3 + 3CH \quad (6.11)$$

$$2C_2S + 4H \rightarrow C_3S_2H_3 + CH \quad (6.12)$$

As a rough estimation of Eq. (6.11a), the reaction yields 0.49 g of CH from 1 g of C_3S and reaction in Eq. (6.11b) yields 0.22 g of CH from 1 g of C_2S. The molecular masses (M) of C_3S, C_2S, and CH are 228, 172, and 74 g/mol, respectively. Thus, the amount of CH generated by hydration reaction is given by balancing the above chemical equations as,

$$CH_{gh}(x,t) = \left[\alpha_{C3S}(t)\left(W_c \frac{\%C_3S}{100}\right)0.49 + \alpha_{C2S}(t)\left(W_c \frac{\%C_2S}{100}\right)0.22\right] A\Delta x \quad (6.13)$$

where W_c is the weight of cement (kg/m^3 of concrete). $\%C_3S$ and $\%C_2S$ are the percentages of C_3S and C_2S in cement, respectively, which can be calculated from the

Bogue's equation. α_{C3S} and α_{C2S} are the degrees of hydration (%) of C_3S and C_2S, respectively, obtained form Tangtermsirikul and Saengsoy (2002). The equations are shown in Appendix A1. A is the cross-sectional area of the element (m^2). Δx is the thickness of the element (m).

(ii) Calcium Hydroxide consumed by pozzolanic reaction

CH liberated from the hydration reaction combines chemically with the reactive component of fly ash to form stable calcium silicates. The components of fly ash are found in both reactively amorphous phases and non-reactively crystallized phases. It is assumed in this model that only the amorphous phase of siliceous component in fly ash is reactive. By making a simple assumption that $C_3S_2H_3$ is the final product of the reaction of CH and SiO_2, the pozzolanic reaction can be simply written as follow.

$$3\ CH \quad + \quad 2\ SiO_2 \quad \rightarrow \quad 3\ C_3S_2H_3 \tag{6.14}$$

From the reaction in Eq. (6.13), 2.52 g of CH (M = 74 g/mol) is utilized by 1 g of SiO_2 (M = 60 g/mol). Thus, the amount of CH consumed by pozzolanic reaction (CH_{cp}) is given by balancing the above chemical equations as,

$$CH_{cp}(x,t) = \left[\alpha_{poz}(t)\left(\phi_f W_f \frac{\%SiO_2}{100}\right)2.52\right]A\Delta x \tag{6.15}$$

where W_f is weight of fly ash in concrete (kg/m^3 of concrete). $\%SiO_2$ is the percentage of SiO_2 in fly ash (obtained from chemical analysis of the fly ash). α_{poz} is degree of pozzolanic reaction of fly ash, obtained from Tangtermsirikul and Saengsoy (2002). The equations are shown in Appendix A2. ϕ_f is the effectiveness ratio of fly ash, which is the weight fraction of the reactive (amorphous) phase of SiO_2 to the total weight of SiO_2 in fly ash. The range of the ratio of amorphous phase of fly ash to the total weight of fly ash was found between 0.6 – 0.9 (Freeman and Carrasquillo 1995, Tikalsky and Carrasquillo 1993). ϕ_f is assumed to be 0.8 for the numerical analysis in this model.

6.4.2 Carbonation Reaction and Its Reaction Rate

The carbonation reaction requires water since carbon dioxide and CH must dissolve and enter the reaction process. In this study, it was assumed that the rate of dissolution of gas in the pore solution follows the Henry's law (Papadakis et al. 1991a, Saeki et al. 1991). Therefore, the concentration of dissolved carbon dioxide in the solution is directly proportional to the partial pressure of the gaseous carbon dioxide above the solution. Since the partial pressure exerted by a gas above the solution can be derived from the ideal gas law, the concentration of dissolved carbon dioxide in the pore solution can be written as follow.

$$[CO_2](x,t) = HRTC(x,t) \tag{6.16}$$

where $[CO_2]$ is the molar concentration of carbon dioxide in pore water (mol/m^3). C is the concentration of carbon dioxide in the gas phase of the pores (mol/m^3). H = 34.2 mol/m^3/atm is the Henry's constant for dissolution of carbon dioxide in water (Papadakis et al. 1991a). R = 8.2×10^{-5} m^3·atm/mol/K (8.3 J/mol/K) is the gas constant. T is

temperature (K). The molar concentration of CH in aqueous phase of the pores can be calculated from,

$$[CH](x,t) = \frac{CH_t(x,t)}{V_w(x,t)} \cdot \frac{1000}{74} \leq [CH]_{sat} \tag{6.17}$$

in which,

$$V_w(x,t) = \left[\frac{C_w(x,t)}{100} \cdot \frac{n(t)}{100}\right] A\,\Delta x \tag{6.18}$$

where [CH] is the molar concentrations of CH in pore water at a specific time and distance from the exposed surface (mol/m^3). $[CH]_{sat}$ is the saturated molar concentration of CH in water (mol/m^3). V_w is the volume of pore water (m^3). CH_t is the total amount of CH (kg), obtained from Eq. (6.10). n is the total porosity (%). C_w is the relative water content (%). A is the considered cross sectional area (m^2). Δx is the thickness of the element (m).

It is rarely that CH is completely dissolved in the pore water. The solubility of the CH in water is very low, which is equal to 25 and 10 mol/m^3 at 0°C and 100°C, respectively (Perry 1997). These values were also assumed in the case of pore solution. Therefore, if the computed value of [CH] from Eq. (3.17) is larger than its concentration at saturated (equilibrium) state, the concentration at equilibrium, $[CH]_{sat}$, is used instead. It is noted that the equilibrium values at other temperatures were derived by a linear interpolation of the values at 0°C and 100°C as follow.

$$[CH]_{sat} = 25 - \frac{15T_c}{100} \tag{6.19}$$

where T_c is the temperature in °C. It is realized that the solubility of CH also depends on the concentration of other ions in the solution, i.e. solubility of CH reduces significantly in solution that has very high concentration of sodium hydroxide (NaOH) and potassium hydroxide (KOH). However, their concentrations in mixture are low and they are carbonated eventually. Thus, at this state, the effect of concentration of other ions on solubility of CH is ignored in the model.

Due to the complexity of the carbonation reactions, the average rate of reaction is applied herein for simplicity. The reaction rate depends on the availability of CH, the concentration of carbon dioxide, and temperature of the pore solution. Based on the Arrhenious's equation for thermically activated process and the assumption that Eq. (6.1) represents the carbonation reaction, the rate of carbonation reaction can be written as follows.

$$r_c(x,t) = k_c\,[CH](x,t)\,[CO_2](x,t) \tag{6.20}$$

in which,

$$k_c = \beta \exp\left[-\frac{E_0}{RT}\right] \tag{6.21}$$

where r_c is the average reaction rate of carbon dioxide with the dissolved CH (the disappearing rate of CH) during the carbonation reaction (mol/m^3/day). k_c is the reaction rate coefficient (m^3/mol/day). R = 8.2×10^{-5} m^3·atm/mol/K (8.3 J/mol/K) is the gas constant. $\beta = 1.9 \times 10^8$ m^3/mol/day is the constant for the reaction. E_0 = 40,000 j/mol is the

activation energy of the reaction. β and E_0 were determined in this study from the trial and error in order to achieve the best accuracy of the prediction of carbonation depth. Consequently, the concentration of CH in the pore solution of the carbonated concrete can be calculated as follow.

$$CH'(x,t) = CH(x,t) - \frac{74\, V_w(x,t)}{1000} \int_0^t r_c(x,t)\, dt \qquad (6.22)$$

where CH' is the amount of CH the carbonated portion of concrete (kg). t is the considered time (day).

6.4.3 pH in Concrete

The concentrations of bases are often expressed in the terms of pH. pH value is determined based on the amount of hydroxyl ion in solution which is obtained from the amount of hydroxyl ion dissociated from CH. Even though the solubility of CH is very low, the soluble part of CH in water is completely ionized. This is because CH is categorized as a strong base. The ionization reaction of CH is given by,

$$Ca(OH)_2 \rightarrow Ca^{2+} + 2\, OH^- \qquad (6.23)$$

The concentration of hydroxyl ion (OH^-) in pore water is twice the concentration of the dissolved CH and is therefore given by,

$$[OH^-](x,t) = 2\, [CH'](x,t) \qquad (6.24)$$

in which

$$[CH'](x,t) = \frac{CH'(x,t)}{V_w(x,t)} \cdot \frac{1000}{74} \qquad (6.23)$$

where $[OH^-]$ and [CH'] are the molar concentrations of OH^- and CH, respectively in concrete pore water (mol/m^3). V_w is the volume of pore water (m^3) obtained from Eq. (6.17). CH' is the amount of CH in the carbonated portion of concrete (kg) obtained from Eq. (6.20). Thereafter the pH value can be computed as follow.

$$pH(x,t) = 14 + \log\{[OH^-](x,t)\} \qquad (6.24)$$

where pH is the pH value of the pore solution.

6.5 Verifications

The results of CH content, used for model verification, were obtained from the test conducted in this study and from Papadakis' (2000). Those test results were determined by TGA method. The test results were compared with the results calculated from the models in Figs. 6.11 and 6.12. It is observed in Fig. 6.11 that the CH content of the cement-only specimen increases with time until a steady state is attained. The CH content of specimens incorporating fly ash (fine aggregate was partially replaced by fly ash) also increases at early age but then drops significantly at later ages due to the pozzolanic reactions. Fig. 6.12 reveals that the CH content of specimens incorporating fly ash (cement was partially replaced by fly ash) at 28 days is smaller than that of the cement-only specimens. The CH

content reduces with the increase of fly ash, mainly due to the reduction of cement content. Trends of the predicted curve are match well with trends of the tested values. The verifications show satisfactory accuracy in predicting the CH concentration.

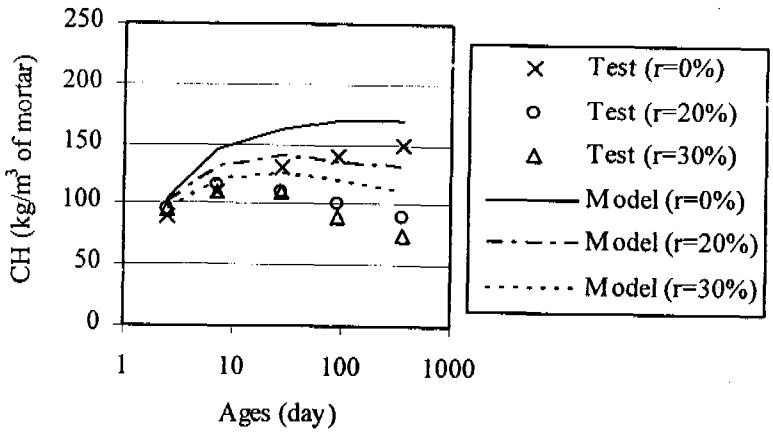

Fig. 6.11 CH in mortar specimen (Papadakis's data): w/b = 0.5 and A/B = 3.0

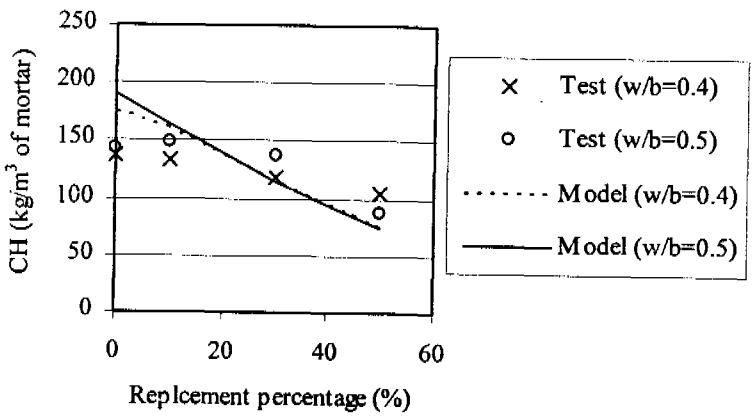

Fig. 6.12 CH in mortar specimen (authors'data) at 28 days (paste volume = 0.50 m^3

The test results of carbonation depth of concrete conducted in this study were used for the verification of pH value. The carbonation depths were determined by spraying on a freshly broken surface with the phenolphthalein solution. The color of the solution changes into purple when pH is higher than the range of approximately nine (RILEM 1988). Therefore, it was assumed in the analysis that the carbonation depth was the distance from the concrete surface to the center of the innermost concrete element that has the pH value less than nine. The comparisons between the carbonation depths of concrete obtained from the test in natural environments and from the models are shown in Figs. 6.13 to 6.16 for the exposure of concrete in city-sheltered, city-non-sheltered, rural, and seaside environments, respectively. It is confirmed that carbonation depth of concrete exposed in the city environment is the highest. For a given fly ash replacement level, a higher w/b led to a greater carbonation depth. When compared with the cement-only concrete, specimens incorporating fly ash exhibited higher carbonation depth. Carbonation depth increases with the increase of fly ash content. Fig. 6.17 presents the overall verification of carbonation depth in various natural environments. The comparisons in Figs. 6.13 to 6.16 and the analytical results in Fig. 6.17 express that the predicted results are in good agreement with the test results of carbonation depth of concrete tested in the natural environments.

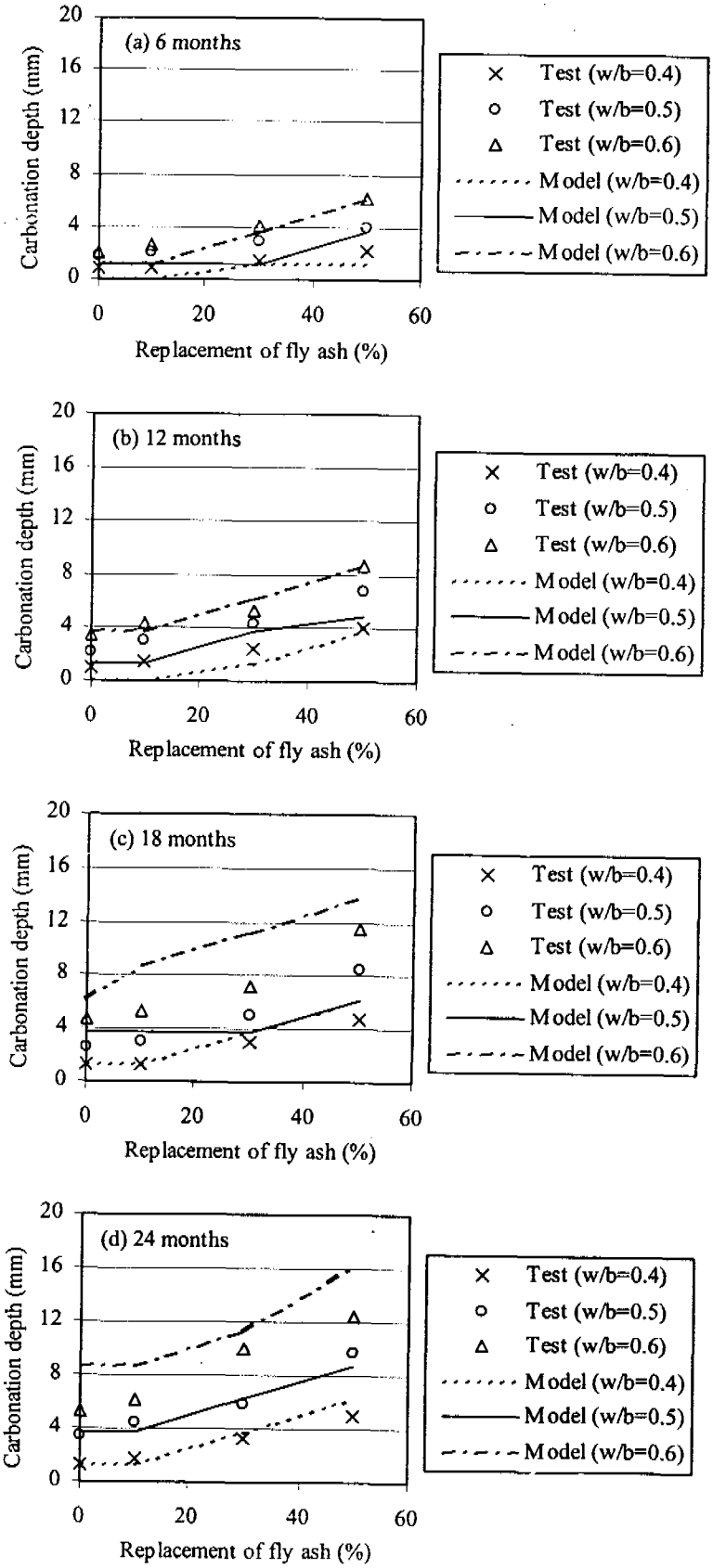

Fig. 6.13 Carbonation depth of concrete tested in city-sheltered environment

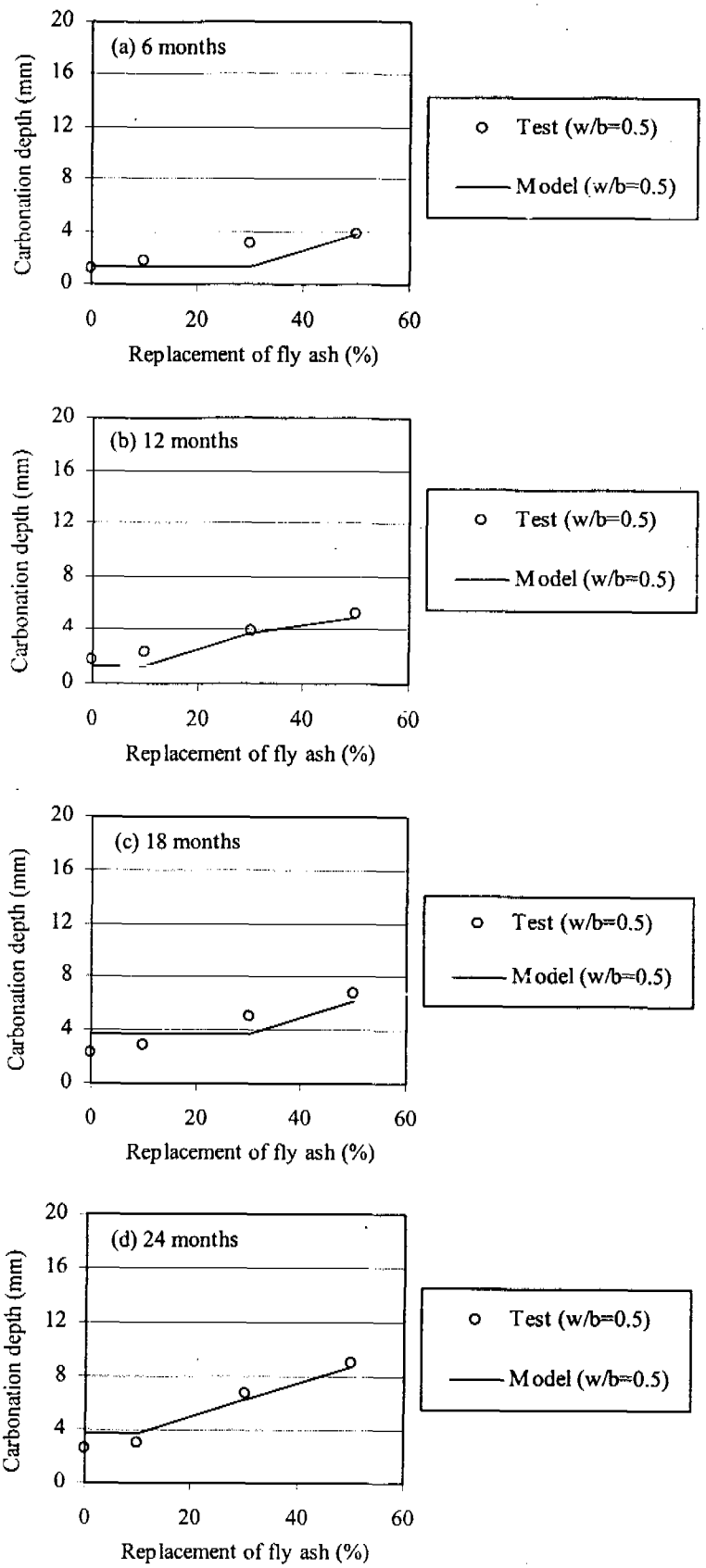

Fig. 6.14 Carbonation depth of concrete tested in city-non-sheltered environment

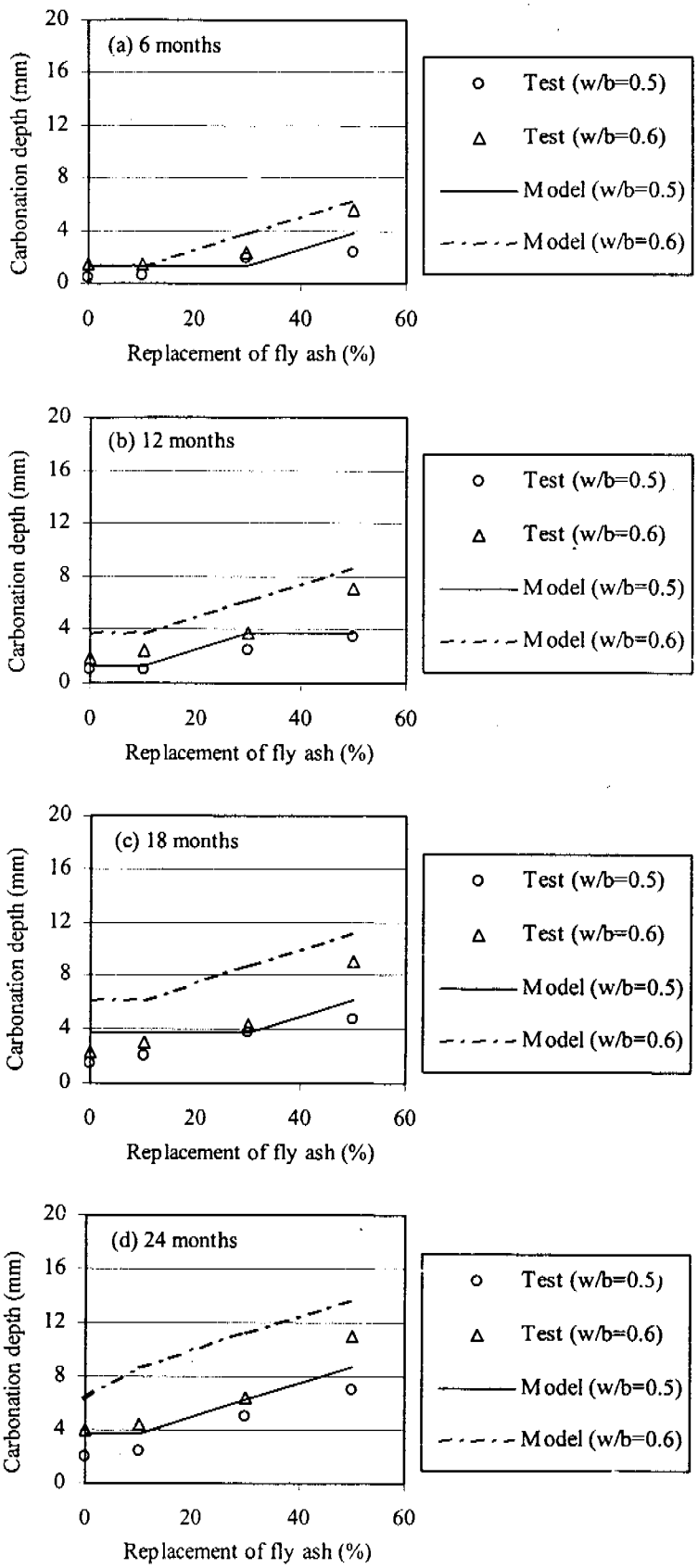

Fig. 6.15 Carbonation depth of concrete tested in rural environment

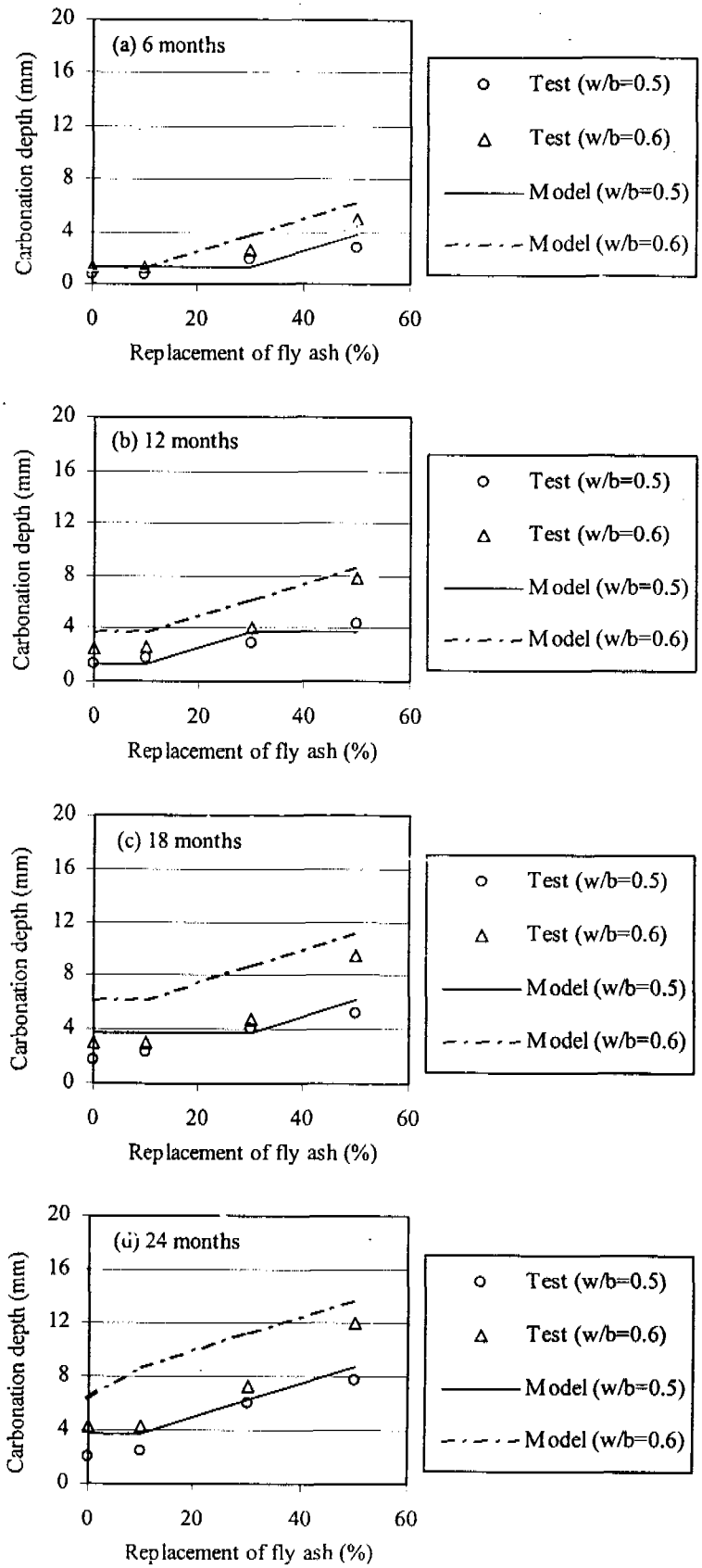

Fig. 6.16 Carbonation depth of concrete tested in seaside environment

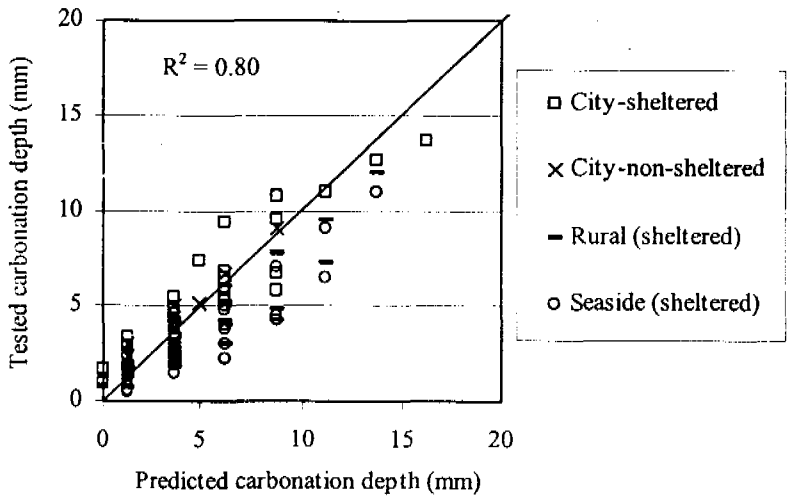

Fig. 6.17 Verification of carbonation depth of concrete tested in natural environments

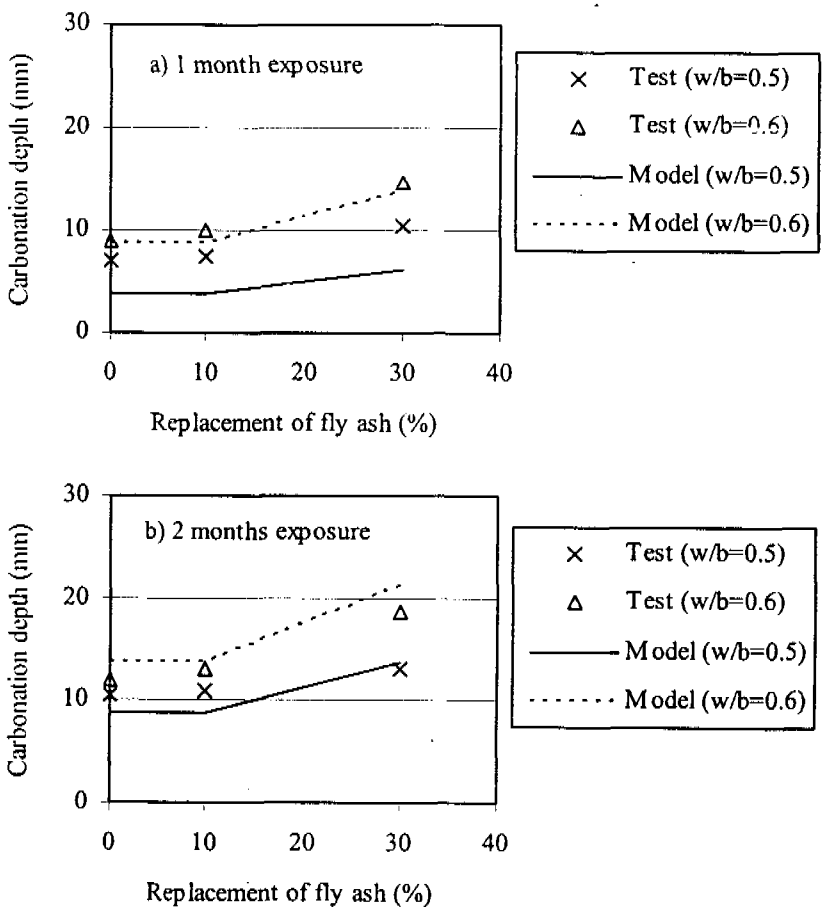

Fig. 6.18 Carbonation depth of concrete tested in accelerated environment (Authors' data)

Moreover, the proposed carbonation simulation model is also verified with the carbonation depths tested in accelerated environment. Fig. 6.18 shows the comparison of test results of carbonation depth of concrete tested in accelerated environment, conducted in this study, with those predicted by the models. The carbon dioxide concentration was 4.0%, temperature was 40 °C, and relative humidity was 55%. Fig. 6.19 presents the comparison of predicted and tested results of carbonation depth conducted by Sulphapa et

al (2003). The carbon dioxide concentration was 6.5%, temperature was 30 °C, and relative humidity was 65%. These comparisons show that the proposed models are also applicable for the carbonation tested in accelerated environment. Fig 6.20 express the verification of carbonation depth in accelerated environments of concretes conducted in this study and by other researchers (Sulphapa, 2003 and Atis 2002). The verification results were also found tc be satisfactory.

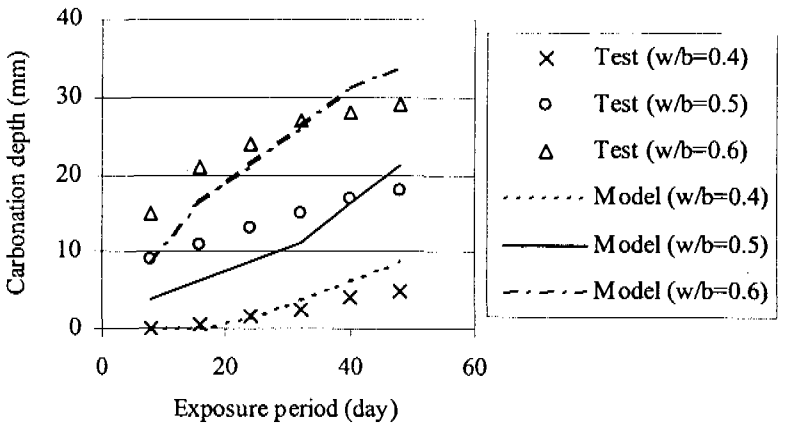

Fig. 6.19 Carbonation depth of concrete tested in accelerated environment (Sulpapha's data)

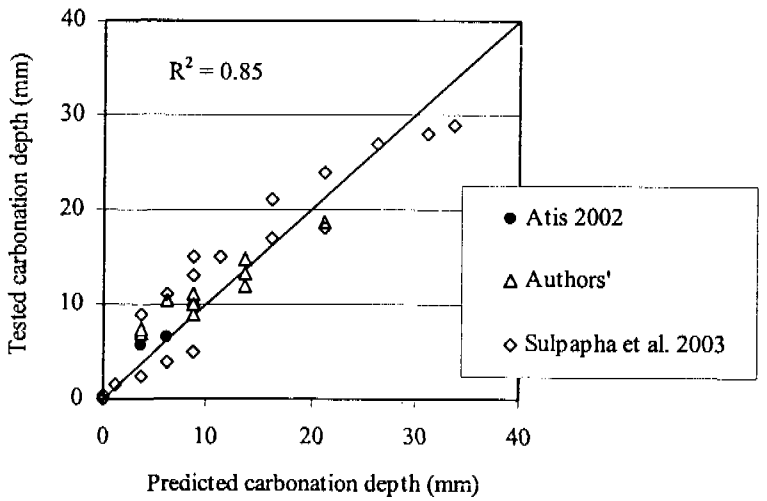

Fig. 6.20 Verification of carbonation depth of concrete in accelerated environment

6.6 Parametric Studies

The proposed carbonation simulation model is parametrically studied to simulate carbonation depth of fly ash concrete in natural environment. Material properties shown in Table 4.1 and 4.2 were used. Concrete mixtures used for simulation were designed to have the γ value of 1.4, and water to binder ratios of 0.3, 0.5, and 0.7. The concrete mixtures were assumed to be cured for 28 days in water before being exposed in carbonation environment for 2 years. Carbon dioxide concentrations in environment are 300 ppm (rural environment), 650 ppm (city environment), and 1000 ppm (severe carbonation environment). The levels of humidity in environment are 60, 75, and 90%. Environmental

temperatures are 20, 30, and 40 °C. The analytical results of carbonation depth of cement only concrete are shown in Figs. 6.21, 6.23, and 6.26 for the effect of carbon dioxide concentration, temperature, and relative humidity, respectively. Figs. 6.22, 6.24, and 6.27 show the analytical results of carbonation depth of fly ash concrete, in which 30% of cement was replaced by fly ash.

6.6.1 Effect of carbon dioxide concentration in environment

The analytical results in Figs. 6.21 and 6.22 show that the calculated carbonation depths increase when the concentration of carbon dioxide in environment increases. These analytical results confirm the test results given in section 5.2.5 that carbonation degree in the city is higher than that in rural and seaside environments, which have lower carbon dioxide concentration.

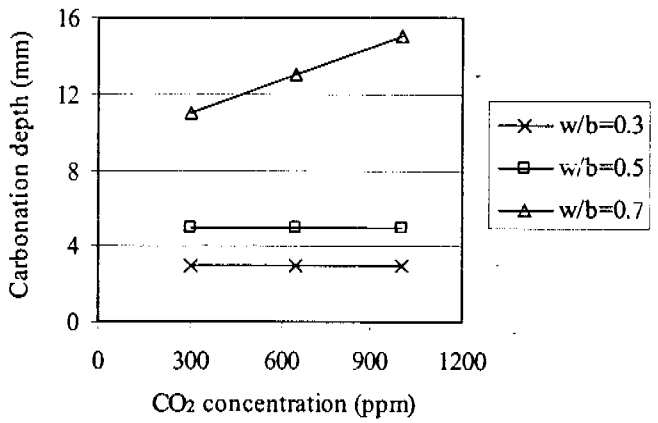

Fig. 6.21 Prediction of carbonation depth of cement only concrete
(Relative humidity = 75% and Temperature = 30 °C)

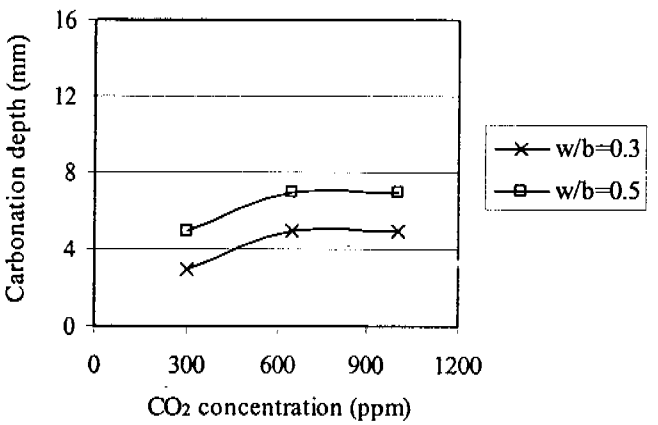

Fig. 6.22 Prediction of carbonation depth of fly ash concrete
(Relative humidity = 75% and Temperature = 30 °C)

6.6.2 Effect of environmental temperature

The analytical results in Figs. 6.23 and 6.24 reveal that the calculated carbonation depth increases when environmental temperature increases. This is because, in hot environment, more amount of pore water transforms into water vapor and the carbonation reaction reacts faster. These analytical results are in agreement with the test results given in

section 5.4.3 that the increase in temperature leads to the increase in carbonation depth (see Fig. 6.25). In addition, it is also noticed in Figs. 6.23 and 6.24 that the effect of environmental temperature becomes less significant for mixture with low water to binder ratio. However, Fig. 6.25 shows adversely that the effect of temperature remains similar for both mixtures with low and high water to binder in accelerated environment.

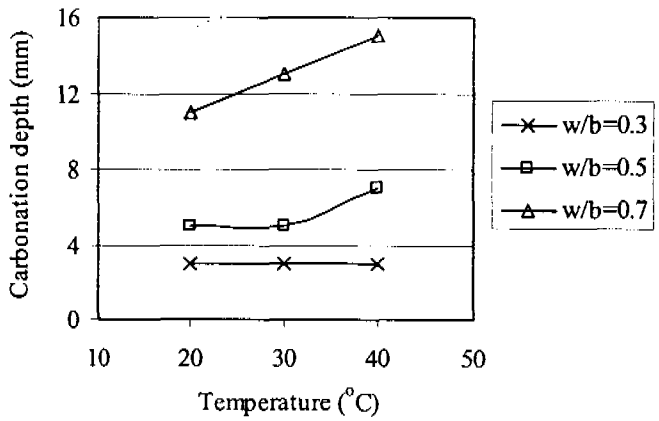

Fig. 6.23 Prediction of carbonation depth of cement only concrete (CO_2 concentration = 650 ppm and Relative humidity = 75%)

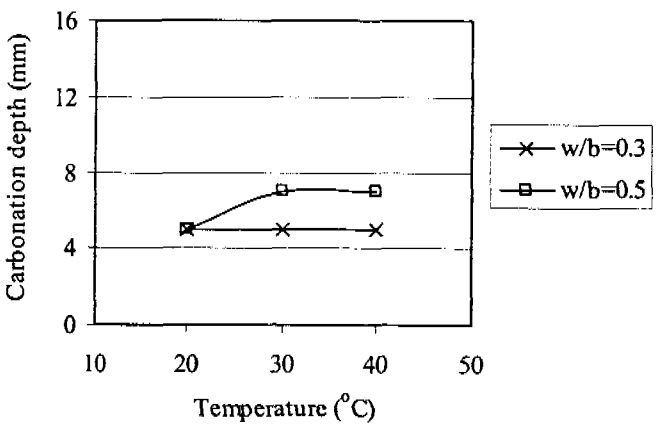

Fig. 6.24 Prediction of carbonation depth of fly ash concrete (CO_2 concentration = 650 ppm and Relative humidity = 75%)

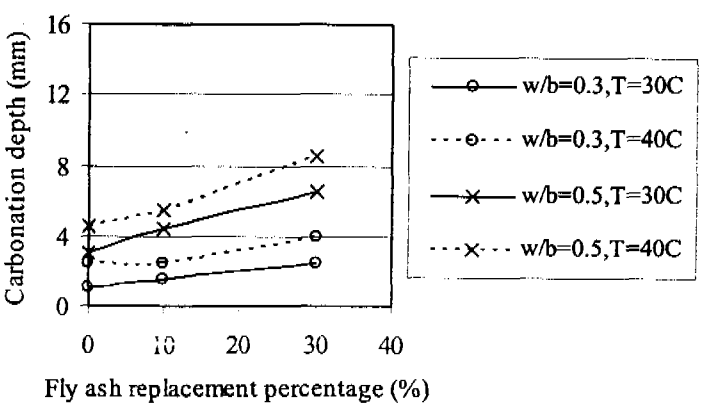

Fig. 6.25 Test result of carbonation depth of mortar in accelerated environment (Effect of environmental temperature)

6.6.3 Effect of environmental humidity

The analytical results in Figs. 6.26 and 6.27 reveal that the calculated carbonation depths decrease when the environmental humidity increases from 60 to 90%. This is because carbonation reaction progresses fast in the semi-humid environment. It is more difficult for gas to penetrate into concrete when the humidity in pores increases, due to a smaller air space in pores. However, it is also noticed that the effect of environmental humidity becomes less significant for cement only mixture with low water to binder ratio. This is in agreement with the test results given in section 5.4.2 that the effect of environmental humidity is less significant for cement only specimens with low water to binder ratio (see Fig. 6.28). This may be because very low diffusion of gas in dense concrete dominates over the effect of relative humidity.

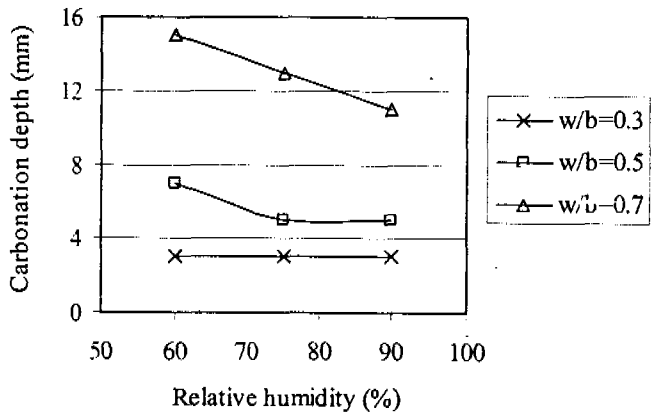

Fig. 6.26 Prediction of carbonation depth of cement only concrete (CO_2 concentration = 650 ppm and Temperature = 30 °C)

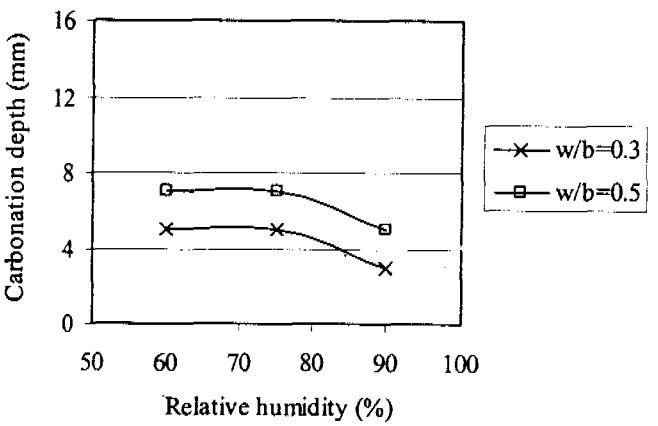

Fig. 6.27 Prediction of carbonation depth of fly ash concrete (CO_2 concentration = 650 ppm and Temperature = 30 °C)

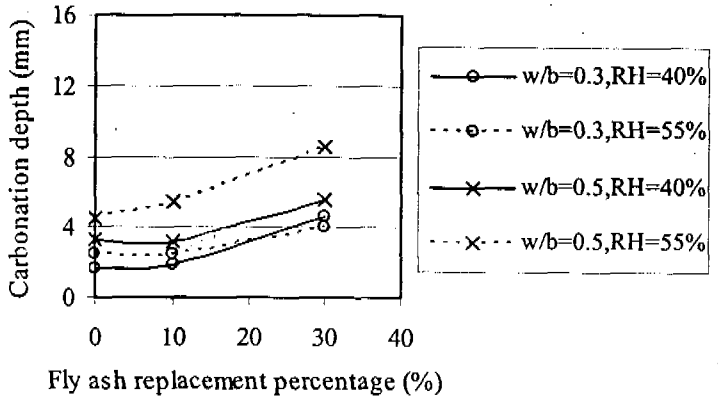

Fig. 6.28 Test result of carbonation depth of mortar in accelerated environment (Effect of relative humidity)